BIOTECHNOLOGY TECHNIQUES
Volume 10 No. 8 (August) pp.573-578
Received as revised 29 May

NEURAL SIMULATION OF AN UNSTEADY STATE CONTINUOUS RECOMBINANT FERMENTATION WITH IMPERFECT MIXING

P. R. Patnaik
Institute of Microbial Technology
Sector 39-A, Chandigarh - 160 036
India

SUMMARY

A continuous fermentation based on a recombinant *Escherichia coli* strain producing tryptophan synthetase has been simulated by a back-propagation neural network. Data for the network were generated through known kinetics applied to a reactor model with an adjustable degree of macromixing of the broth. A network with just one hidden layer performed satisfactorily for both poor and good macromixing. The best performance was at an intermediate level of mixing, in the region of maximum productivity of the recombinant protein.

INTRODUCTION

Industrial fermentations utilising genetically modified microorganisms are complex and difficult to model accurately. They have structural and segregational instabilities (Montague and Morris,1994), and are sensitive to the mixing character of the broth and the influx of disturbances (Patnaik,1993a; 1994a; 1995a). These features and strict sterility requirements make it difficult to have reliable on-line measurements of the fermentation broth.

In the absence of good models and *in vitro* measurement techniques for large scale fermentations, neural networks offer convenient and reliable on-line estimates, predict the effects of disturbances and provide corrective action (Di Massimo *et al.*,1992; Linko and Zhu,1992; Montague *et al.*,1992). They learn from the data, improve with usage and do not require a process model. Recent applications to glucoamylase (Linko and Zhu,1992), ethanol (Karim and Rivera,1992) and penicillin (Montague *et al.*,1992) fermentations, and to the growth of microorganisms (Syu and Tsao,1993; Ye *et al.*,1994; Zhang *et al.*,1994) attest the usefulness of neural simulations.

Despite the growing importance of rDNA-based processes, only a few of these applications pertain to recombinant strains. Ye and coworkers(1994) showed that a combination of two fuzzy neural networks could increase β-glucosidase production four-fold in *Escherichia coli* harboring the plasmid pUR2921. With a different *E. coli* strain containing a plasmid coding for glyceraldehyde-3-phosphate dehydrogenase, Patnaik(1995b) showed that a radial basis network could faithfully predict the start-up behavior in the presence of disturbances.

Neural networks for recombinant fermentations have so far not considered imperfect mixing of the broth. Recent work (Patnaik 1993b; 1994a,b) has shown that perfect mixing is not always desirable and that there are optimal degrees of micromixing and macromixing that maximise the yield of the recombinant protein. The optimal degree may change as fermentation progresses, and hence it is important to sense or estimate the variables affected by the state of mixing and control the manipulated parameters dynamically. This communication assesses the ability of a neural network to learn from performance data and mimic a recombinant fermentation in an impefectly mixed bioreactor.

MATHEMATICAL ANALYSIS

Macromixing is often more significant than micromixing in large bioreactors, and its influence increases with the size of the vessel and the growth of biomass (Ruggeri and Sassi, 1993). This inference is also supported by the observation

that the relaxation times for cellular metabolism may be two to three orders of magnitude larger than for fluid mixing (Roels, 1983).

The present study is based on a batch reactor model proposed by Tanner *et al.*(1985). They conceptualised the broth to consist of two well-mixed regions with the outflow of each region being fed into the other. Each region thus functions as a continuous flow bioreactor but, as there is no overall exchange of fluid with the surroundings, the combination simulates a batch environment. The degree of macromixing is controlled by the recycle (or dilution) rates; perfect mixing is approached at large dilution rates while a dilution rate close to zero approximates plug flow.

The Tanner model has been generalised and extended to a continuous flow bioreactor (Fig. 1). First, Tanner and coworkers assumed that the dilution rates, and therefore the degrees of macromixing, in the two mixing regions were equal; this restriction has been removed. Secondly, because of the flow there is an overall dilution rate, which may be related to the two internal dilution rates. These three dilution rates are:

$$D_1 = (Q + R)/V_1 \tag{1}$$

$$D_2 = (Q + R)/V_2 \tag{2}$$

$$D = Q/(V_1 + V_2) \tag{3}$$

From eqs.(1) to (3) it follows that:

$$Q/V_1 = D(1 + D_1/D_2) \tag{4}$$

$$R/V_1 = D_1 - D(1 + D_1/D_2) \tag{5}$$

$$Q/V_2 = D(1 + D_2/D_1) \tag{6}$$

$$R/V_2 = D_2 - D(1 + D_2/D_1) \tag{7}$$

$$(1/D_1) + (1/D_2) = (1/D)[Q/(Q + R)] \tag{8}$$

Large values of D_1 and D_2 promote good mixing; because they are internal to the bioreactor there is no risk of washout, which can occur if D exceeds a threshold value.

The reaction system chosen was the production of tryptophan synthetase, secreted by an *E. coli* M12K12ΔH1Δtrp strain hosting the plasmid pPLc23trpA1. The organism and the kinetics have been described elsewhere (Park *et al.*, 1991). Incorporation of the kinetic equations in the mixing model of Fig. 1 results in the equations given below for the unsteady state performance of a continuous fermentation.

$$\frac{dy_1}{dt} = [D_1 - D(1 + \frac{D_1}{D_2})]y_6 - D_1 y_1 + (1 - \theta)\mu_1^+ y_1 \tag{9}$$

$$\frac{dy_2}{dt} = [D_1 - D(1 + \frac{D_1}{D_2})]y_7 - D_1 y_2 + \theta\mu_1^+ y_1 + \mu_1^- y_2 \tag{10}$$

$$\frac{dy_3}{dt} = [D_1 - D(1 + \frac{D_1}{D_2})]y_8 + D(1 + \frac{D_1}{D_2}) - D_1 y_3$$

$$-(\mu_1^+ y_1 + \mu_1^- y_2).\frac{X_1^+(0)}{Y_x S(0)} - \frac{X_1^+(0)}{S(0)Y_p}.\frac{dy_4}{dt} \tag{11}$$

$$\frac{dy_4}{dt} = [D_1 - D(1 + \frac{D_1}{D_2})]y_9 - D_1 y_4 + \epsilon y_5 y_1[(1-\theta)\mu_1^+ + a] - k_p y_4 \quad (12)$$

$$\frac{dy_5}{dt} = [D_1 - D(1 + \frac{D_1}{D_2})]y_{10} - D_1 y_5 + \frac{b y_5 \mu_1^+}{(c + y_5)(d + \mu_1^+)} \quad (13)$$

$$\frac{dy_6}{dt} = D_2(y_1 - y_6) + (1-\theta)\mu_2^+ y_6 \quad (14)$$

$$\frac{dy_7}{dt} = D_2(y_2 - y_7) + \theta\mu_2^+ y_6 + \mu_2^- y_7 \quad (15)$$

$$\frac{dy_8}{dt} = D_2(y_3 - y_8) - \frac{X_1^+(0)}{S(0)Y_x}(\mu_2^+ y_6 + \mu_2^- y_7) - \frac{X_1^+(0)}{S(0)Y_p}\frac{dy_9}{dt} \quad (16)$$

$$\frac{dy_9}{dt} = D_2(y_4 - y_9) + \epsilon y_{10} y_6[(1-\theta)\mu_2^+ + a] - k_p y_9 \quad (17)$$

$$\frac{dy_{10}}{dt} = D_2(y_5 - y_{10}) + \frac{b y_{10}\mu_2^+}{(c + y_{10})(d + \mu_2^+)} \quad (18)$$

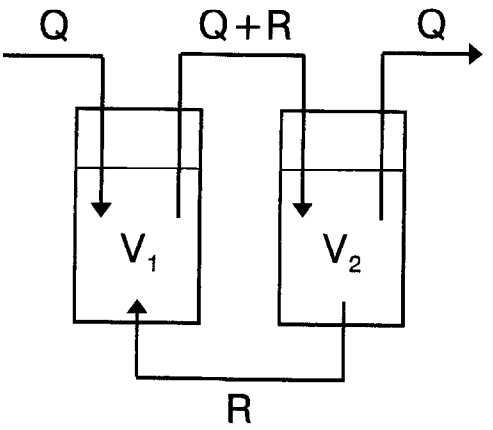

Fig.1. Conceptual two-region model of macromixing in a continuous flow bioreactor.

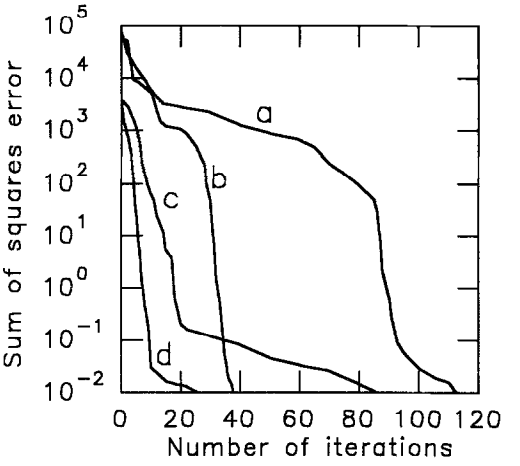

Fig.2. Performance of the neural network for different degrees of macromixing as training progresses.

The specific growth rates of both plasmid-containing cells and plasmid-free cells follow Monod kinetics but at different rates.

$$\mu_1^+ = \frac{\mu_{1m}^+ y_3}{K_m^+/S(0) + y_3}; \mu_1^- = \frac{\mu_{1m}^- y_3}{K_m^-/S(0) + y_3}$$

$$\mu_2^+ = \frac{\mu_{2m}^+ y_8}{K_m^+/S(0) + y_8}; \mu_2^- = \frac{\mu_{2m}^- y_8}{K_m^-/S(0) + y_8}$$

In many bioreactor designs the feed is introduced close to the impeller blades as this helps good dispersion (Mayr *et al.*, 1992). Therefore the first reactor in Fig. 1 corresponds to the region near the impeller, while the second reactor depicts the outer region, from which the outlet stream is usually drawn. Since the medium is aqueous and the initial cell mass concentration is small (about 1 to 2%), the starting culture may be assumed to be homogeneous. To maximise productivity the starting culture should have no plasmid-free cells. Then, from the definitions of the $y_j (j = 1, 2, ..., 10)$ in the Notation, their initial conditions should be:

$$y_1(0) = 1; y_2(0) = 0; y_3(0) = 1; y_4(0) = 0; y_6(0) = 1; y_7(0) = 0; y_8(0) = 1; y_9(0) = 0.$$

The initial conditions for y_5 and y_{10}, which are the intra-cellular plasmid concentrations (g plasmid DNA/g cells), were set at 0.001 from previous work (Park *et al.*, 1991; Patnaik, 1993b). In keeping with normal operating practice, the feed is assumed to be sterile.

NEURAL SIMULATION

Data to train the neural network were generated by solving eqs.(9) to (18) with the parameter values and starting concentrations used previously (Patnaik, 1993b). Different combinations of the dilution rates D_1, D_2 and D were employed so as to simulate both poor and good mixing in each region. Since $R/V_1 > 0$ and $R/V_2 > 0$, eqs.(5) and (7) prescribe an upper limit for D for a given choice of D_1 and D_2. In other words, unlike a perfectly mixed reactor, the washout dilution rate depends on the degree of mixing as well as the specific growth rate.

Earlier studies (Linko and Zhu, 1992; Montague *et al.*, 1992; Zhang *et al.*, 1994) suggest that a three-layer feed-forward neural network trained by the back-propagation algorithm is suitable. The first layer receives and transmits the inputs, which are the initial conditions for $y_j (j = 1, 2, ..., 10)$; the second layer has the hidden neurons, and the third is the output layer. The number of neurons in the first and third layers are equal to the number of input and output variables respectively, each ten in this problem. The number of hidden neurons was increased sequentially until a specified convergence criterion was achieved (Di Massimo *et al.*, 1992); in particular, the sum of the squares of the differences between the training data and the predicted data over an operating period of 15 hours was reduced to below 0.01. Based on previous studies (Linko and Zhu, 1992; Zhang *et al.*, 1994), a sigmoidal transfer function was employed for the hidden layer and a linear transformation for the output layer.

Whereas constant input vectors may be employed in static simulations, in a dynamic simulation the network uses the process data at each time step to predict the values at the next step (Di Massimo *et al.*, 1992; Zhang *et al.*, 1994). Hence the input vectors were sampled from the transient fermentation data but they were one time-step behind the target data, i.e. the predicted performance. As simple backpropagation was not adequate, it was improved by adaptive learning with Levenberg-Marquardt minimisation, which has been effective even with Gaussian noise (Thibault *et al.*, 1990).

Representative results are displayed in Figs. 2 to 4. Cases (a) and (b) represent poor macromixing while the other two are for good macromixing. Figure 2 shows how the performance of the neural network progressed with training. The minimum numbers of hidden neurons required to reach the specified accuracy are the values at which the plots meet the abcissa. The plots indicate that, for a given degree of macromixing in the impeller region (i.e. for a specified D_1), the network learns the bioreactor performance with fewer trials and fewer hidden nodes for a poorly mixed peripheral region (small D_2) than for a well-mixed one. Comparison of plots (a) and (d) of both figures, however, indicates that improved mixing in

the impeller region (large D_1) enables the network to learn the performance faster. These two contrasting features imply that the network's peak efficiency is at an intermediate level of macromixing. Since such an intermediate level also maximises recombinant production formation (Patnaik, 1993b;1994b), the results of this initial study suggest the suitability of a feed-forward network for a recombinant fermentation with plasmid instability and imperfect mixing.

While Figs. 2 and 3 indicate the overall performance of the neural network, Fig. 4 shows the accuracies of predictions for the concentrations of the two kinds of cells and of tryptophan synthetase in the two mixing regions. The mean absolute percentage deviation (MAPD) is defined as:

$$\text{MAPD} = \frac{\Sigma_{i=1}^{M}[|(\text{test value} - \text{network prediction})|/\text{test value}]_i}{M} * 100$$

where M is the number of sampling points in time. In this study the data were sampled at half hour intervals over a 15 hour period. Despite the small number of data, the network predictions were accurate, the maximum MAPD being 2.07%.

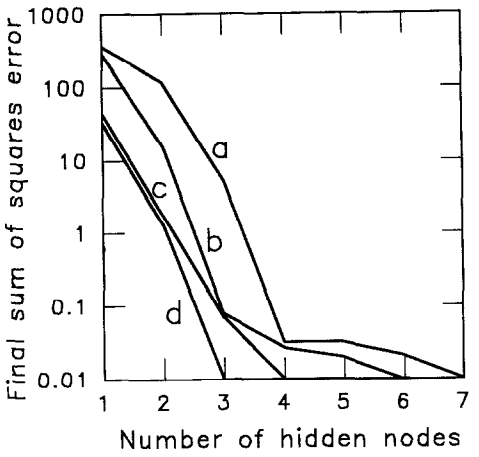

Fig.3. Dependence of simulation accuracy of the neural network on the number of hidden nodes for different degrees of macromixing.

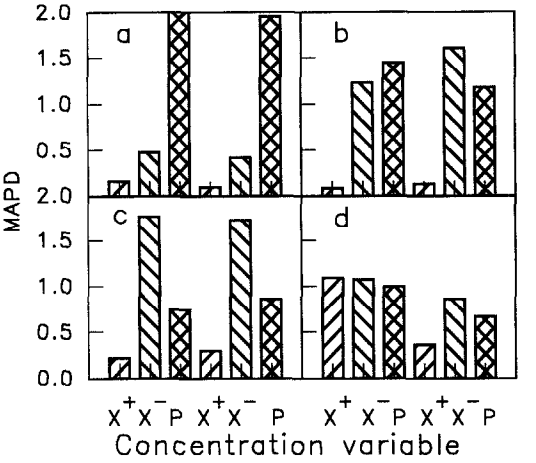

Fig.4. Mean absolute percentage errors in network predictions of fermentation variables. Note: The left set of [X^+X^-P] corresponds to region1 and the right set to region2.

NOTATION

a, b, c, d	constants, h^{-1},h^{-1},g g^{-1}, h^{-1}
D	dilution rate of the bioreactor, h^{-1}
D_i	internal dilution rate of region i (i=1,2), h^{-1}
G_i	intracellular plasmid concentration, (g plasmid DNA) (g cells)$^{-1}$
k_p	product decay constant, h^{-1}
K_m^+	Monod constant for plasmid-bearing cells, g l^{-1}
K_m^-	Monod constant for plasmid-free cells, g l^{-1}
P_i	tryptophan concentration in region i (i=1,2), g l^{-1}
Q	inflow or outflow rate, g l^{-1}
R	internal recycle rate, g l^{-1}
S_i	substrate concentration in region i (i=1,2), g l^{-1}

$S(0)$	initial concentration of substrate, g l^{-1}
t	time, h
V_i	volume of region i (i=1,2), l
X_i^+	concentration of plasmid-bearing cells in region i (i=1,2), g l^{-1}
X_i^-	concentration of plasmid-free cells in region i (i=1,2), g l^{-1}
$X_1^+(0)$	initial concentration of plasmid-bearing cells, g l^{-1}
Y_p	yield coefficient of product, -
Y_x	yield coefficient of biomass, -
y_1, y_6	X_1^+(or X_2^+)$/X_1^+(0)$, -
y_2, y_7	X_1^-(or X_2^-)$/X_1^+(0)$, -
y_3, y_8	S_1(or S_2)$/S(0)$, -
y_4, y_9	P_1(or P_2)$/X_1^+(0)$, -
y_5, y_{10}	G_1, G_2, -
Greek letters	
ϵ	gene expression efficiency, -
θ	plasmid loss probability, -
μ_i^+	specific growth rate of plasmid-containing cells in region i (i=1,2), h^{-1}
μ_i^-	specific growth rate of plasmid-free cells in region i (i=1,2), h^{-1}
μ_{im}^+	maximum value of μ_i^+ (i=1,2), h^{-1}
μ_{im}^-	maximum value of μ_i^- (i=1,2), h^{-1}

REFERENCES

DiMassimo, C., Lant, P., Saunders, A., Montague, G.A., Tham, M.T. and Morris, A.J.(1992). *J. Chem. Technol. Biotechnol.* **53**, 265-277.

Karim, M.N. and Rivera, S.L.(1992). *Adv. Biochem. Eng./Biotechnol.* **46**, 1-33.

Linko, P. and Zhu, Y.-H.(1992). *Process Biochem.* **27**, 275-283.

Mayr, B., Horvat, P. and Moser, A.(1992). *Bioprocess Eng.* **8**, 137-143.

Montague, G.A. and Morris, A.J.(1994). *Trends Biotechnol.* **12**, 312-324.

Montague, G.A., Morris, A.J. and Tham, M.T.(1992). *J. Biotechnol.* **25**, 183-201.

Park, S.H., Ryu, D.D.Y. and Lee, S.B.(1991). *Biotechnol. Bioeng.* **37**, 404-414.

Patnaik, P.R.(1993a). *Biotechnol. Techniques* **7**, 137-142.

Patnaik, P.R.(1993b). *Chem. Eng. Commun.* **125**, 155-169.

Patnaik, P.R.(1994a). *J. Chem. Technol. Biotechnol.* **61**, 337-342.

Patnaik, P.R.(1994b). *Indian Chem. Engr.* **36**, 85-88.

Patnaik, P.R.(1995a). *Chem. Eng. Commun.* **131**, 125-140.

Patnaik, P.R.(1995b). *Biotechnol. Techniques* **9**, 691-696.

Roels, J.A.(1983). *Energetics and Kinetics in Biotechnology*, Elsevier Biomedical, Amsterdam, pp.205-221.

Ruggeri, B. and Sassi, G.(1993). *Chem. Eng. Commun.* **122**, 1-56.

Ryu, D.D.Y., Kim, J.-Y. and Lee, S.B.(1991). In *Biotechnology* (Ed. K. Schugerl), Vol.4, VCH, Weinheim, pp.485-505.

Syu, M.-J. and Tsao, G.T.(1993). *Biotechnol. Bioeng.* **42**, 376-380.

Tanner, R.D., Dunn, I.J., Bourne, J.R. and Klu, M.K.(1985). *Chem. Eng. Sci.* **40**, 1213-1219.

Thibault, J., van Breusegem, V. and Cheruy, A.(1990). *Biotechnol. Bioeng.* **36**, 1041-1048.

Ye, K., Jin, K.Y. and Shimizu, K.(1994). *J. Ferment. Bioeng.* **77**, 663-673.

Zhang, Q., Reid, J.F., Litchfield, J.B., Ren, J. and Chang, S.-W.(1994). *Biotechnol. Bioeng.* **43**, 483-489.